Use of Rapid-Scan EPR to Improve Detection Sensitivity for Spin-Trapped Radicals

Deborah G. Mitchell,[†‡] Gerald M. Rosen,[¶‖††] Mark Tseitlin,[†‡] Breanna Symmes,[§] Sandra S. Eaton,[†‡] and Gareth R. Eaton[†‡*]

[†]Department of Chemistry and Biochemistry, [‡]Center for EPR Imaging in Vivo Physiology, and [§]Department of Biological Sciences, University of Denver, Denver, Colorado; and [¶]Center for EPR Imaging in Vivo Physiology, [‖]Center for Biomedical Engineering and Technology, and [††]Department of Pharmaceutical Sciences, University of Maryland, Baltimore, Maryland

ABSTRACT The short lifetime of superoxide and the low rates of formation expected in vivo make detection by standard continuous wave (CW) electron paramagnetic resonance (EPR) challenging. The new rapid-scan EPR method offers improved sensitivity for these types of samples. In rapid-scan EPR, the magnetic field is scanned through resonance in a time that is short relative to electron spin relaxation times, and data are processed to obtain the absorption spectrum. To validate the application of rapid-scan EPR to spin trapping, superoxide was generated by the reaction of xanthine oxidase and hypoxanthine with rates of 0.1–6.0 μM/min and trapped with 5-*tert*-butoxycarbonyl-5-methyl-1-pyrroline-N-oxide (BMPO). Spin trapping with BMPO to form the BMPO-OOH adduct converts the very short-lived superoxide radical into a more stable spin adduct. There is good agreement between the hyperfine splitting parameters obtained for BMPO-OOH by CW and rapid-scan EPR. For the same signal acquisition time, the signal/noise ratio is >40 times higher for rapid-scan than for CW EPR. Rapid-scan EPR can detect superoxide produced *by Enterococcus faecalis* at rates that are too low for detection by CW EPR.

INTRODUCTION

Superoxide ($O_2^{\bullet -}$) is well known for its role in the Fenton reaction and oxidative stress (1–3). It is generated by a broad spectrum of enzymes and has been shown to be an important cell-signaling agent, controlling a variety of physiological functions (3,4). Yet our knowledge of these signaling events is currently based only on in vitro models. For example, we have shown that $O_2^{\bullet -}$ generated by the metabolism of xanthine by xanthine oxidase can promote the germination of *Bacillus anthracis* endospores (5). Similar findings were obtained using activated macrophages (6). Although these models are highly suggestive of an important cell-signaling role for $O_2^{\bullet -}$, it has not been possible to confirm the analogous pathways in vivo. Improving the sensitivity of detection of $O_2^{\bullet -}$ requires improved methods. The research described herein is an important step toward detecting $O_2^{\bullet -}$ in cells by electron paramagnetic resonance (EPR).

Reactive oxygen species, including hydroxyl ($HO^{\bullet}$) and superoxide ($O_2^{\bullet -}$) radicals, have lifetimes at ambient temperature that are too short to be detected directly by EPR. The spin-trapping technique, in which a short-lived radical reacts with a nitrone or nitroso compound to form a more stable radical (Scheme 1), was developed in the late 1960s (7,8). For many years, 5,5-dimethyl-1-pyrroline-N-oxide (DMPO) (Scheme 1) was the nitrone of choice for detecting $O_2^{\bullet -}$ and $HO^{\bullet}$ because of the characteristic EPR spectra of the adducts DMPO-OOH and DMPO-OH (9,10). DMPO has played a pivotal role in identifying $O_2^{\bullet -}$ in many enzymatic reactions, including nitric oxide synthases (11–14). More recently, spin traps have been synthesized with either a diethoxyphosphoryl (DEPMPO) (15) or ester group, such as 5-*tert*-butoxycarbonyl-5-methyl-1-pyrroline-N-oxide (BMPO) (16–18). BMPO (Scheme 1) has a larger rate constant for trapping $O_2^{\bullet -}$ than DMPO, and BMPO-OOH exhibits a longer half-life than DMPO-OOH (18). However, even with improvements in spin traps, the low rate of formation of $O_2^{\bullet -}$ in vivo makes detection by EPR extremely challenging.

Continuous-wave (CW) EPR has been the method of choice for most spin-trapping experiments. Analogously to NMR, Fourier transform (FT) EPR has the potential to improve the sensitivity of EPR. However, electron spin relaxation times are orders of magnitude shorter than nuclear spin relaxation times, which limits the utility of FT-EPR. Electron spin relaxation times for spin-trapped radicals are expected to be similar to those for the more stable nitroxides. Although T_2 for rapidly tumbling nitroxides in deoxygenated aqueous solutions is ~0.5 μs (19), unresolved hyperfine splittings and collisions with O_2 reduce T_2* (the effective decay time for a free induction decay) to <100 ns. These short T_2* values are less than the dead time of most pulsed EPR spectrometers, which drastically reduces detected signal intensity and makes the signal/noise ratio (S/N) per unit time for FT-EPR spectra of spin-trapped radicals poorer than that for CW.

We propose that a novel (to our knowledge) detection method, rapid-scan EPR, can substantially improve the sensitivity of EPR for detection of spin-trapped radicals. In a rapid-scan experiment, the magnetic field is scanned through resonance in a time that is short relative to electron

Submitted May 4, 2013, and accepted for publication June 4, 2013.

*Correspondence: geaton@du.edu

Editor: Betty Gaffney.

© 2013 by the Biophysical Society

0006-3495/13/07/0338/5 $2.00

http://dx.doi.org/10.1016/j.bpj.2013.06.005

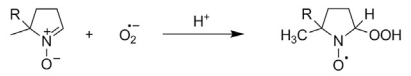

R = CH_3, DMPO
R = $P(O)(OEt)_2$, DEPMPO
R = $CO_2C(CH_3)_3$, BMPO

R = CH_3, DMPO-OOH, $t_{1/2}$=66 s @ pH 7.4
R = $P(O)(OEt)_2$, DEPMPO-OOH, $t_{1/2}$=18 min @ pH 7.0
R = $CO_2C(CH_3)_3$, BMPO-OOH, $t_{1/2}$= 22 min @ pH 7.4

SCHEME 1 Spin-trapping reagents and reaction. The half-lives cited in this scheme are from Tsai et al. (18), Frejaville et al. (15), and Rosen et al. (43).

spin relaxation times. The absorption and dispersion signals are recorded by direct detection with a double-balanced mixer instead of by phase-sensitive detection at the modulation frequency, as is used in conventional CW spectroscopy. Rapid-scan signals can be deconvolved to give the slow-scan absorption spectrum (20,21). Rapid-scan EPR was initially developed at 250 MHz for applications to in vivo imaging (22–24). A historical perspective of the method is provided in Stoner et al. (22). The direct detection of the absorption spectrum distinguishes the method used in this study from earlier studies in which the term "rapid scan" indicated faster scans than were available with commercial instrumentation, but still used phase-sensitive detection at the modulation frequency. More recently, X-band (9.5 GHz) rapid-scan EPR was shown to provide a dramatically improved S/N for the E′ defect in irradiated fused quartz (25), for paramagnetic defects in amorphous hydrogenated silicon and in diamonds (26), and for nitroxides in fluid solution (27). X-band rapid-scan EPR also is useful for characterizing the distributions of relaxation times for α,γ-bisdiphenylene-β-phenylallyl (BDPA) (28).

In this work, we demonstrate the improvement in S/N for BMPO-OOH recorded by rapid-scan EPR relative to CW EPR. The oxidation of hypoxanthine by xanthine oxidase was used as a continuous enzymatic source of $O_2^{\bullet -}$, with rates of generation in the range of 0.1–6 μM/min. To demonstrate applicability to a living organism, we used rapid-scan EPR with BMPO as the spin trap to detect $O_2^{\bullet -}$ produced by *Enterococcus faecalis. E. faecalis* is a human intestinal commensal that has been shown to produce extracellular $O_2^{\bullet -}$ (29). Rapid-scan EPR spectroscopy, combined with the best of the current generation of spin traps, permits characterization of the $O_2^{\bullet -}$ generated at rates similar to those that would be observed in isolated cells, in short periods of time that permit temporal resolution of the signal. The low concentrations of BMPO-OOH that can be observed by rapid-scan EPR are undetectable by CW EPR.

MATERIALS AND METHODS

The BMPO spin trap was synthesized as described in the literature (18). Xanthine oxidase (EC 1.1.3.22), hypoxanthine, superoxide dismutase (SOD), horse heart ferricytochrome *c*, and diethylenetriaminepentaacetic acid (DTPA) were purchased from Sigma-Aldrich (St. Louis, MO). *E. faecalis* ATTC strain 19443 was purchased from Carolina Biological Supply (Burlington, NC). Brain-heart infusion agar (BHI) was purchased from Fischer Scientific (Philadelphia, PA). Samples for EPR spectroscopy were contained in 0.8 mm inner diameter Pyrex capillaries supported in 4 mm outer diameter quartz EPR tubes.

To validate the method, we generated $O_2^{\bullet -}$ using hypoxanthine and xanthine oxidase at pH 7.4 (30). Typically, xanthine oxidase (0.04 U/mL) was added to pH ~7.4 sodium phosphate buffer (50 mM) containing DTPA (1 mM) and hypoxanthine (0.5–400 μM, final concentration) to achieve rates of $O_2^{\bullet -}$ formation that ranged from 0.1 to 6.0 μM/min. We estimated the superoxide formation rate by monitoring the SOD-inhibitable reduction of ferricytochrome c (80 μM) at room temperature (31). Spin trapping was performed by addition of 100 mM BMPO in pH ~7.4 phosphate-buffered saline (PBS; 50 mM) containing 1 mM DTPA to the solution of hypoxanthine and xanthine oxidase to achieve a final BMPO concentration of 50 mM in the reaction mixture. EPR spectra were recorded 10 min after mixing reagents. The half-life of BMPO-OOH at ambient temperature is reported to be ~23 min (18). Solutions for control experiments contained SOD (30 U/mL).

The procedure for growing *E. faecalis* for spin-trapping experiments was similar to that described in the literature (32–34). The *E. faecalis* was incubated at 37°C for 16 h in aqueous BHI media. After samples were spun at 8600 RCF for 2 min, the bacteria-containing pellets were washed with PBS and resuspended in PBS. We estimated the rate of formation of $O_2^{\bullet -}$ by *E. faecalis* in the presence of 10 mM glucose to be 0.1 nmoles/min per 1.0×10^6 colony-forming units (CFU) by monitoring the SOD-inhibitable reduction of ferricytochrome c (80 μM) at room temperature. Bacteria were enumerated by two methods: 1), the optical density (O.D.) at 620 nm was measured at several different dilutions, and a molar absorptivity of 2.0×10^9 CFU O.D.$^{-1}$ mL^{-1} was used to convert OD to CFU; and 2), each suspension of bacteria was further diluted by a factor of 100,000 and 10 μL was plated on BHI. The individual colonies that formed overnight (at 37°C) were counted to determine the average number of CFU/mL.

CW EPR spectra were obtained on a Bruker EMX-plus X-band (9.5 GHz) EPR spectrometer (Bruker, Billerica, MA) with a super high quality factor (SHQ) resonator. With these samples in the resonator, the Q was ~3000 and the resonator efficiency ($B_1/\sqrt{W}$) was 1.2 (26,27). Although the peak-to-peak first-derivative line widths for individual hyperfine lines were ~0.75 G, the spectra were overmodulated with modulation amplitude ~0.75 G. The 20 mW microwave power (B_1 = 170 mG) was too high to be in the regime where signal amplitude increases linearly with the square root of power. High modulation amplitude and microwave power were used to maximize the signal amplitude, although these parameters broaden the lines and decrease resolution of the small hyperfine splittings.

Rapid-scan EPR spectra were obtained on a custom Bruker E500T X-band spectrometer with a dielectric ER4118X-MD5 resonator. In the dielectric resonator, the B_1 excites spins over a sample height of ~1 cm, which is about half as large as in the SHQ resonator. In comparing the performance of CW and rapid-scan EPR, we did not take this factor of ~2 difference in the number of spins detected into account. The samples lowered the resonator Q, as measured with a locally designed addition to the bridge (35), to ~850. We determined the efficiency of the resonator by measuring the dependence of signal amplitude on $\sqrt{P}$ for an aqueous sample of the stable nitroxide 4-hydro-3-carbamoyl-2,2,5,5-tetra-perdeuteromethyl-pyrrolin-1-^{15}N-oxyl (^{15}N-mHCTPO), and simulating the power saturation curve with the program SATMON (36) using known values of T_1, T_2, and unresolved proton hyperfine couplings (27). Sinusoidal scans were generated with a locally designed and built scan driver (37) that includes interchangeable capacitors to resonate the scan-coil circuit. Litz wire coils with 7.6 cm average diameter were mounted outside the resonator, coaxially with the main magnetic field. The scan frequency was ~51 kHz and the scan widths were 55 G. The signal amplitude for BMPO-OOH changes too rapidly with time to permit acquisition of a power saturation curve. Based on the power saturation behavior for stable nitroxides in aqueous solution (27), a microwave power of ~53 mW (B_1 = 250 mG) was selected to maximize the signal amplitude with <2% line broadening. Data were acquired in segments containing one to 12 cycles of the sinusoidal scans.

These segments were averaged 100 k times. Background correction (38), sinusoidal deconvolution (20), combination of signals in real and imaginary channels, and combination of up-field and down-field scans were performed to obtain the spectra shown in Figs. 1–3.

A fourth-order Butterworth filter was applied to both the CW and rapid-scan data to decrease noise. The filter parameter was selected to broaden the signals by <2%.

RESULTS AND DISCUSSION

CW spectra of BMPO-OOH were obtained with a Bruker X-band (9.5 GHz) EMX Plus and a SHQ resonator that represents the current state of the art. Rapid-scan spectra were recorded on a custom Bruker X-band E500T with a dielectric resonator. The dielectric resonator is advantageous for rapid-scan experiments because the rapidly changing magnetic fields induce fewer eddy currents compared with the SHQ resonator. CW and rapid-scan spectra were obtained for BMPO-OOH produced by 6 μM/min generation of $O_2^{\bullet -}$ from hypoxanthine/xanthine oxidase (Fig. 1). The conventional first derivative spectrum and the first integral of the CW spectrum are shown in Fig. 1, *A* and *B*, respectively. Fig. 1 *C* is the deconvolved rapid-scan spectrum, which was obtained in 10% of the time required for the CW spectrum (Fig. 1 *A*). Rapid-scan spectra are presented as the absorption signal because that is the form in which data are recorded. Both CW and rapid-scan spectra for BMPO-OOH exhibited the characteristic 12-line pattern that arises from nearly equal hyperfine splittings by one nitrogen with A_N = 13.23 G and one proton with A_H = 11.8 G, and nearly equal populations of two isomers (18). There is good agreement between the nuclear hyperfine splittings observed in the CW and rapid-scan spectra (18). The smaller splittings are better resolved in the rapid-scan absorption spectrum (Fig. 1 *C*) than in the first integral of the CW spectrum (Fig. 1 *B*) because the high modulation amplitude and power used to obtain the CW spectrum broadened the lines. Because magnetic field modulation is not used to record the rapid scan spectrum, this source of line broadening is avoided. For comparison of the two methods, the spectra in Fig. 1 were obtained with approximately the same B_1. Because the time on resonance is shorter for rapid-scan than for CW EPR, a higher microwave B_1 can be used without causing power broadening (27), which improves the S/N for rapid-scan EPR.

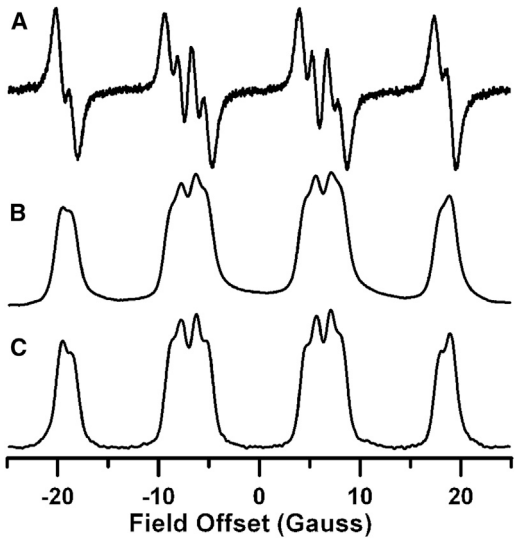

FIGURE 1 Comparison of CW and rapid-scan spectra of BMPO-OOH in solution with a $O_2^{\bullet -}$ production rate of 6 μM/min, recorded 10 min after mixing reagents. The $O_2^{\bullet -}$ was produced by a hypoxanthine/xanthine oxidase mixture. (*A*) CW spectrum obtained with 55 G sweep width, 0.75 G modulation amplitude, single 42 s scan, 20 ms time constant, and 20 mW (B_1 = 170 mG) microwave power. (*B*) The first integral of the spectrum in panel *A*. (*C*) Deconvolved rapid-scan spectrum obtained with 55 G scan width, 51 kHz scan frequency, 20 mW (B_1 = 150 mG) microwave power, 100 k averages with one cycle averaged, and a total time of ~4 s.

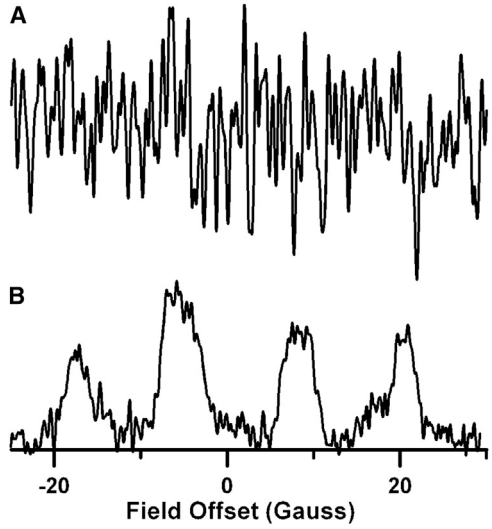

FIGURE 2 Comparison of CW and rapid-scan spectra of BMPO-OOH in solution with a $O_2^{\bullet -}$ production rate of 0.1 μM/min, recorded 10 min after mixing reagents. The $O_2^{\bullet -}$ was produced by a hypoxanthine/xanthine oxidase mixture. The concentration of BMPO-OOH is ~0.3 μM. (*A*) CW spectrum obtained with 55 G sweep width, 0.75 G modulation amplitude, single 30 s scan, 15 ms conversion time, 10 ms time constant, and 20 mW (B_1 = 170 mG) microwave power. (*B*) Deconvolved rapid-scan spectrum obtained with 55 G scan width, 51 kHz scan frequency, and 53 mW (B_1 = 250 mG) microwave power. Segments consisting of 12 sinusoidal cycles were averaged 100 k times, with a total data acquisition time of ~30 s.

CW and rapid-scan spectra in Fig. 2 were obtained in 30 s of data acquisition time for samples with formation rates of 0.1 μM/min $O_2^{\bullet -}$, which is 60 times lower than the rate in Fig. 1. In the CW spectrum (Fig. 2 *A*), there is barely a hint of the BMPO-OOH signal. By contrast, the rapid-scan spectrum recorded in the same 30 s of data acquisition time has an S/N of ~10 (Fig. 2 *B*). Based on the comparison in Fig. 2, it is evident that rapid-scan EPR permits detection of BMPO-OOH with good lineshape fidelity at low production rates than are inaccessible by CW EPR for the same data acquisition time. The ability of rapid-scan EPR to acquire higher S/N data in a shorter time than CW will improve

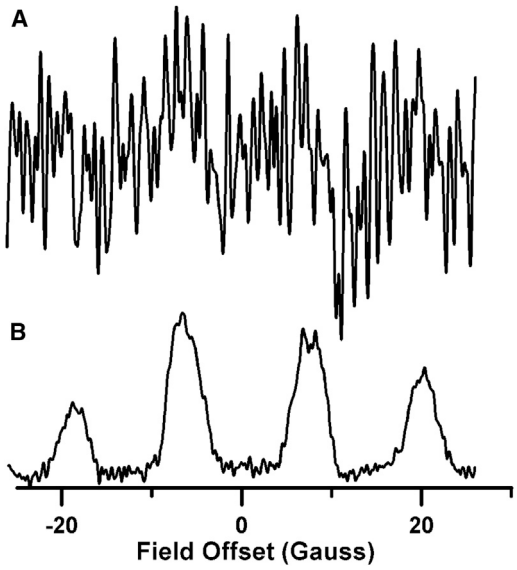

FIGURE 3 Comparison of CW and rapid-scan spectra of BMPO-OOH in a suspension of *E. faecalis* with 2×10^6 CFU/mL and a $O_2^{\bullet -}$ production rate of 0.2 μM/min, recorded 10 min after mixing reagents. The concentration of BMPO-OOH is ~0.5 μM. (*A*) CW spectrum obtained with 55 G sweep width, 0.75 G modulation amplitude, single 30 s scan, 15 ms conversion time, 10 ms time constant, and 20 mW (B_1 = 170 mG) microwave power. (*B*) Deconvolved rapid-scan spectrum obtained with 55 G scan width, 51 kHz scan frequency, and 53 mW (B_1 = 250 mG) microwave power. Segments consisting of 12 sinusoidal cycles were averaged 100 k times, with a total data acquisition time of ~30 s.

the temporal resolution of spin-trapping experiments and be crucial for in vivo imaging.

Rapid-scan EPR was applied to a bacterial system, the extracellular production of $O_2^{\bullet -}$ by *E. faecalis*, at a rate of 0.1 nmoles/min per 1.0×10^6 CFU (Fig. 3). At this rate of $O_2^{\bullet -}$ production, it was difficult to determine whether the EPR spectrum of BMPO-OOH was present in a CW spectrum with 30 s acquisition time (Fig. 3 *A*). By contrast, the characteristic BMPO-OOH signal in a rapid-scan spectrum with a 30 s acquisition time has an S/N of ~42 (Fig. 3 *B*). The data in Fig. 3 demonstrate the improved sensitivity of rapid-scan relative to CW EPR in a living system.

There are several reasons why rapid-scan EPR yields better S/N than CW EPR: 1) In every scan, the full amplitude of the signal is detected by rapid-scan EPR, in contrast to conventional spectroscopy, where the signal amplitude that is detected is limited by the modulation amplitude and increasing the modulation amplitude causes broadening of the line. 1) In the rapid-scan spectrum, the magnetic field is on resonance for a shorter period of time than in the conventional CW spectrum, so higher microwave power can be used without saturation of the signal (22,25,27). 3) In the rapid scans, the absorption and dispersion signals are combined, which gives up to a $\sqrt{2}$ improvement in S/N (39). The net result of these factors is a major improvement in S/N that is especially important at low radical concentrations. As shown in Figs. 2 and 3, improved S/N can make the difference between detecting and not detecting an EPR signal. In addition, if the S/N is the same, we can calculate the number of spins from the absorption spectrum about twice as accurately as we could from the first derivative signal (40).

CONCLUSIONS

The experiments described here demonstrate that rapid-scan EPR can detect lower concentrations of BMPO-OOH radicals than can be detected by CW EPR. The improvement in S/N for BMPO-OOH that can be obtained by rapid-scan compared with CW EPR is applicable to many radicals with relaxation times that are too short for pulsed EPR, including other types of nitroxides. With the development of low-frequency EPR spectrometers with imaging capability (41,42), nitroxides can serve important roles in the study of physiology. We envision that rapid-scan EPR will become an integral component of future EPR imagers, and will expand opportunities to apply spin-trapping and stable nitroxides to explore important physiologic questions in vivo, in situ, and in real time.

We thank Dr. Scott Barbee (Department of Biology, University of Denver) for allowing us to use his BSL-2 hood and other materials.

This work was supported by grants from the National Institutes of Health (P41 grant EB002034 to G.M.R. and G.R.E. [H. Halpern, PI], and EB002807 and EB000557 to G.R.E. and S.S.E.) and the National Science Foundation (IDBR 0753018 to G.R.E. and S.S.E.). D.G.M. received a graduate fellowship from the National Science Foundation.

REFERENCES

1. Görlach, A., R. P. Brandes, …, R. Busse. 2000. A gp91phox containing NADPH oxidase selectively expressed in endothelial cells is a major source of oxygen radical generation in the arterial wall. *Circ. Res.* 87:26–32.
2. Hensley, K., K. A. Robinson, …, R. A. Floyd. 2000. Reactive oxygen species, cell signaling, and cell injury. *Free Radic. Biol. Med.* 28:1456–1462.
3. Rodrigues, J. V., and C. M. Gomes. 2012. Mechanism of superoxide and hydrogen peroxide generation by human electron-transfer flavoprotein and pathological variants. *Free Radic. Biol. Med.* 53:12–19.
4. Buetler, T. M., A. Krauskopf, and U. T. Ruegg. 2004. Role of superoxide as a signaling molecule. *News Physiol. Sci.* 19:120–123.
5. Baillie, L., S. Hibbs, …, G. M. Rosen. 2005. Role of superoxide in the germination of Bacillus anthracis endospores. *FEMS Microbiol. Lett.* 245:33–38.
6. Raines, K. W., T. J. Kang, …, G. M. Rosen. 2006. Importance of nitric oxide synthase in the control of infection by Bacillus anthracis. *Infect. Immun.* 74:2268–2276.
7. Janzen, E. G., and B. J. Blackburn. 1968. Detection and identification of short-lived free radicals by an electron spin resonance trapping technique. *J. Am. Chem. Soc.* 90:5909–5910.
8. Chalfont, G. R., M. J. Perkins, and A. Horsfield. 1968. A probe for hemolytic reactions in solution. II. The polymerization of styrene. *J. Am. Chem. Soc.* 90:7141–7142.

9. Harbour, J. R., and J. R. Bolton. 1975. Superoxide formation in spinach chloroplasts: electron spin resonance detection by spin trapping. *Biochem. Biophys. Res. Commun.* 64:803–807.
10. Finkelstein, E., G. M. Rosen, and E. J. Rauckman. 1980. Spin trapping. Kinetics of the reaction of superoxide and hydroxyl radicals with nitrones. *J. Am. Chem. Soc.* 102:4994–4999.
11. Pou, S., L. Keaton, …, G. M. Rosen. 1999. Mechanism of superoxide generation by neuronal nitric-oxide synthase. *J. Biol. Chem.* 274:9573–9580.
12. Pou, S., W. S. Pou, …, G. M. Rosen. 1992. Generation of superoxide by purified brain nitric oxide synthase. *J. Biol. Chem.* 267:24173–24176.
13. Xia, Y., L. J. Roman, …, J. L. Zweier. 1998. Inducible nitric-oxide synthase generates superoxide from the reductase domain. *J. Biol. Chem.* 273:22635–22639.
14. Vásquez-Vivar, J., B. Kalyanaraman, …, K. A. Pritchard, Jr. 1998. Superoxide generation by endothelial nitric oxide synthase: the influence of cofactors. *Proc. Natl. Acad. Sci. USA.* 95:9220–9225.
15. Fréjaville, C., H. Karoui, …, P. Tordo. 1994. 5-Diethoxyphosphoryl-5-methyl-1-pyrroline N-oxide (DEPMPO): a new phosphorylated nitrone for efficient in vitro and in vivo spin trapping of oxygen-centred radical. *J. Chem. Soc. Chem. Commun.* 1793–1794.
16. Zhang, H., J. Joseph, …, B. Kalyanaraman. 2000. Detection of superoxide anion using an isotopically labeled nitrone spin trap: potential biological applications. *FEBS Lett.* 473:58–62.
17. Stolze, K., N. Udilova, …, H. Nohl. 2003. Synthesis and characterization of EMPO-derived 5,5-disubstituted 1-pyrroline N-oxides as spin traps forming exceptionally stable superoxide spin adducts. *Biol. Chem.* 384:493–500.
18. Tsai, P., K. Ichikawa, …, G. M. Rosen. 2003. Esters of 5-carboxyl-5-methyl-1-pyrroline N-oxide: a family of spin traps for superoxide. *J. Org. Chem.* 68:7811–7817.
19. Biller, J. R., V. Meyer, …, G. R. Eaton. 2011. Relaxation times and line widths of isotopically-substituted nitroxides in aqueous solution at X-band. *J. Magn. Reson.* 212:370–377.
20. Tseitlin, M., G. A. Rinard, …, G. R. Eaton. 2011. Deconvolution of sinusoidal rapid EPR scans. *J. Magn. Reson.* 208:279–283.
21. Joshi, J. P., J. R. Ballard, …, G. R. Eaton. 2005. Rapid-scan EPR with triangular scans and Fourier deconvolution to recover the slow-scan spectrum. *J. Magn. Reson.* 175:44–51.
22. Stoner, J. W., D. Szymanski, …, G. R. Eaton. 2004. Direct-detected rapid-scan EPR at 250 MHz. *J. Magn. Reson.* 170:127–135.
23. Tseitlin, M., T. Czechowski, …, G. R. Eaton. 2008. Regularized optimization (RO) reconstruction for oximetric EPR imaging. *J. Magn. Reson.* 194:212–221.
24. Tseitlin, M., A. Dhami, …, G. R. Eaton. 2007. Comparison of maximum entropy and filtered back-projection methods to reconstruct rapid-scan EPR images. *J. Magn. Reson.* 184:157–168.
25. Mitchell, D. G., R. W. Quine, …, G. R. Eaton. 2011. Comparison of Continuous Wave, Spin Echo, and Rapid Scan EPR of Irradiated Fused Quartz. *Radiat. Meas.* 46:993–996.
26. Mitchell, D. G., M. Tseitlin, …, G. R. Eaton. 2013. X-band rapid-scan EPR of samples with long electron relaxation times: a comparison of continuous wave, pulse, and rapid-scan EPR. *Mol. Phys.* 10.1008/00268976.2013.792959.
27. Mitchell, D. G., R. W. Quine, …, G. R. Eaton. 2012. X-band rapid-scan EPR of nitroxyl radicals. *J. Magn. Reson.* 214:221–226.
28. Mitchell, D. G., R. W. Quine, …, G. R. Eaton. 2011. Electron spin relaxation and heterogeneity of the 1:1 α,γ-bisdiphenylene-β-phenylallyl (BDPA)/benzene complex. *J. Phys. Chem. B.* 115:7986–7990.
29. Huycke, M. M., W. Joyce, and M. F. Wack. 1996. Augmented production of extracellular superoxide by blood isolates of Enterococcus faecalis. *J. Infect. Dis.* 173:743–746.
30. Fridovich, I. 1985. Xanthine oxidase. *In* CRC Handbook of Methods for Oxygen Radical Research. R. A. Greenwald, editor. CRC Press, Boca Raton. 51–53.
31. Kuthan, H., V. Ullrich, and R. W. Estabrook. 1982. A quantitative test for superoxide radicals produced in biological systems. *Biochem. J.* 203:551–558.
32. Moore, D. R., Y. Kotake, and M. M. Huycke. 2004. Effects of iron and phytic acid on production of extracellular radicals by Enterococcus faecalis. *Exp. Biol. Med. (Maywood).* 229:1186–1195.
33. Huycke, M. M., V. Abrams, and D. R. Moore. 2002. Enterococcus faecalis produces extracellular superoxide and hydrogen peroxide that damages colonic epithelial cell DNA. *Carcinogenesis.* 23:529–536.
34. Huycke, M. M., D. Moore, …, M. S. Gilmore. 2001. Extracellular superoxide production by Enterococcus faecalis requires demethylmenaquinone and is attenuated by functional terminal quinol oxidases. *Mol. Microbiol.* 42:729–740.
35. Quine, R. W., D. Mitchell, and G. R. Eaton. 2011. A general purpose Q-measuring circuit using pulse ring-down. *Concepts Magn. Reson. Part B Magn. Reson. Eng.* 39B:43–46.
36. Rakowsky, M. H., A. Zecevic, …, S. S. Eaton. 1998. Determination of high-spin iron(III)-nitroxyl distances in spin-labeled porphyrins by time-domain EPR. *J. Magn. Reson.* 131:97–110.
37. Quine, R. W., D. G. Mitchell, …, G. R. Eaton. 2012. A resonated coil driver for rapid scan EPR. *Concepts Magn. Reson. Part B Magn. Reson. Eng.* 41B:95–110.
38. Tseitlin, M., D. G. Mitchell, …, G. R. Eaton. 2012. Corrections for sinusoidal background and non-orthogonality of signal channels in sinusoidal rapid magnetic field scans. *J. Magn. Reson.* 223:80–84.
39. Tseitlin, M., R. W. Quine, …, G. R. Eaton. 2010. Combining absorption and dispersion signals to improve signal-to-noise for rapid-scan EPR imaging. *J. Magn. Reson.* 203:305–310.
40. Tseitlin, M., S. S. Eaton, and G. R. Eaton. 2012. Uncertainty analysis for absorption and first-derivative EPR spectra. *Concepts Magn. Reson.* 40A:295–305.
41. Caia, G. L., O. V. Efimova, …, J. L. Zweier. 2012. Organ specific mapping of in vivo redox state in control and cigarette smoke-exposed mice using EPR/NMR co-imaging. *J. Magn. Reson.* 216:21–27.
42. Bézière, N., C. Decroos, …, Y.-M. Frapart. 2012. First combined in vivo X-ray tomography and high-resolution molecular electron paramagnetic resonance (EPR) imaging of the mouse knee joint taking into account the disappearance kinetics of the EPR probe. *Mol. Imaging.* 11:220–228.
43. Rosen, G. M., B. E. Britigan, …, S. Pou. 1999. Free Radicals: Biology and Detection by Spin Trapping. Oxford University Press, New York. p. 339.